# Dynamics of noncontact rack-and-pinion device: Periodic back-and-forth motion of the rack

Mojtaba Nasiri,[1] Ali Moradian,[1] and MirFaez Miri[2,*]
[1]*Institute for Advanced Studies in Basic Sciences (IASBS), P.O. Box 45195-1159, Zanjan 45195, Iran*
[2]*Department of Physics, University of Tehran, P.O. Box 14395-547, Tehran, Iran*
(Received 4 July 2010; published 1 September 2010)

We study a nanoscale system composed of one corrugated cylinder (pinion) and one corrugated plate (rack). The pinion and rack have no mechanical contact, but are coupled via the lateral Casimir force. We consider the case where the rack position versus time is a periodic triangular signal. We find that the device can rectify the periodic but nonsinusoidal motion of the rack. Using the typical values of parameters, we find that the pinion rotates with an average angular velocity $\Omega = 1 \sim 100$ Hz. Experimental observation of the pinion rotation will show that the quantum vacuum can intermesh the noncontact parts of nanomachines.

DOI: 10.1103/PhysRevE.82.037101 PACS number(s): 07.10.Cm, 85.85.+j, 42.50.Lc, 46.55.+d

## I. INTRODUCTION

As a key interaction at nanoscale, the Casimir force [1,2] influences the dynamics of small devices. Chan and collaborators have experimentally demonstrated frequency shifts, hysteretic behavior, and bistability caused by the Casimir force in the frequency response of a periodically driven micromachined torsional oscillator [3].

Two sinusoidally corrugated surfaces experience the *lateral* Casimir force, as has been predicted [4,5] and verified experimentally [6]. Recently it has been suggested that the lateral Casimir force may intermesh the noncontact parts of nanomechanical devices [7–11]. This gives a partial solution to the wear problem in nanoscale mechanical systems [12].

Ashourvan, Miri, and Golestanian studied a rack and pinion with no contact but coupled via the quantum vacuum. The pinion is subject to an external load and experiences friction when rotates around its axis. It is shown that both *uniform* [8] and *sinusoidal* [9] motion of the rack can be converted into uniform motion of the load. In this Brief Report, we consider the case where the rack position versus time is a periodic triangular signal. There are three reasons for our study. First, from an experimental point of view, it seems easier to enforce a rack to undergo a bidirectional rather than a unidirectional motion. Realization of a high velocity unidirectional motion requires a rack of great length. Second, it is an immediate question whether the device can rectify periodic but nonsinusoidal motion of the rack. Third, we focus on a heavily damped system, so that inertia can be neglected. We show explicitly that the rectified motion of the pinion is a consequence of the inherent *nonlinearity* of the system.

Here, we consider the noncontact rack and pinion device shown schematically in Fig. 1(a). Two harmonically corrugated plates with identical wavelength $\lambda$ and lateral displacement $x-y$ experience a lateral Casimir force $F_{\text{lateral}} = -F \sin[\frac{2\pi}{\lambda}(x-y)]$. The amplitude of the lateral Casimir force depends on the distance $H$ between the pinion and rack, corrugation wavelength $\lambda$, corrugation amplitudes $a_p$ and $a_r$, and radius $R$ [4,5,8]. Recently, the (lateral) Casimir force in a variety of complex geometries have gained much attention, see e.g., [13–18]. The Casimir torque plays the key role in the equation of motion

$$-RF \sin\left[\frac{2\pi}{\lambda}(x-y)\right] - \frac{\zeta}{R}\frac{dx}{dt} - rW = 0 \qquad (1)$$

for the coordinate $x = R\theta$, where $\theta$ is the angle of rotation and $\zeta$ is the rotational friction coefficient. In the overdamped motion of the pinion, $\lambda$ and $\zeta\lambda/(FR^2)$ are the natural units of length and time, respectively. We define the scaled variables $X = x/\lambda$, $Y = y/\lambda$, and $T = FR^2 t/(\zeta\lambda)$. We assume that the rack position $y$ versus time $t$ is a periodic triangular signal as shown in Fig. 1(b). The periodic signal can be characterized with the parameters $y_0$, $T_*$, $T_1$, and $S_1$. In its first period

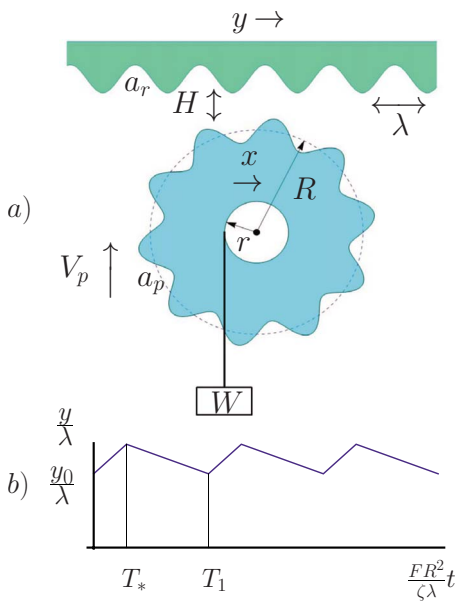


FIG. 1. (Color online) (a) The schematics of the rack and pinion device. The pinion and rack have sinusoidal corrugations of wavelength $\lambda$ and amplitudes $a_p$ and $a_r$, respectively. The rectified motion of the pinion manifests in a positive average velocity $V_p$, while working against an external load $W$. (b) The rack position versus time is a periodic triangular signal, characterized by $y_0$, $T_*$, $T_1$, and $S_1$.

*miri@iasbs.ac.ir

 

$$y=\begin{cases} y_0+S_1FR^2t/\zeta & 0<\dfrac{FR^2t}{\zeta\lambda}<T_*, \\ y_0-\lambda S_2T_1+S_2FR^2t/\zeta & T_*<\dfrac{FR^2t}{\zeta\lambda}<T_1. \end{cases} \tag{2}$$

Here $S_2=S_1T_*/(T_*-T_1)$. Note that the average velocity $\langle dy/dt\rangle$ is zero.

## II. PERIODIC SOLUTIONS

Introducing $Z=Y-X=(y-x)/\lambda$, the equation of motion can be rewritten as [19]

$$\frac{dZ}{dT}+\sin(2\pi Z)=\begin{cases} \dfrac{Wr}{FR}+S_1 & 0<\mathrm{mod}(T,T_1)<T_*, \\ \dfrac{Wr}{FR}+S_2 & T_*<\mathrm{mod}(T,T_1)<T_1. \end{cases} \tag{3}$$

This maps the pinion dynamics to the dynamics of overdamped Josephson junction driven by a square wave pulse [20]. The analytical solutions of $dZ/dT+\sin(2\pi Z)=I$ for $I>1$ and $I<1$ are

$$T-T_0=\frac{1}{\pi\sqrt{I^2-1}}\arctan\left(\frac{I\tan(\pi Z)-1}{\sqrt{I^2-1}}\right),$$

$$T-T_0=\frac{1}{2\pi\sqrt{1-I^2}}\ln\left|\frac{I\tan(\pi Z)-1-\sqrt{1-I^2}}{I\tan(\pi Z)-1+\sqrt{1-I^2}}\right|, \tag{4}$$

respectively. Here $T_0$ is an integration constant. Note that in case of $I<1$, $Z=\frac{1}{2\pi}\arcsin I$ is a stable fixed point, while $Z=\pm\frac{1}{2}-\frac{1}{2\pi}\arcsin I$ is an unstable fixed point. If the initial value $Z(0)$ falls into $[\frac{1}{2\pi}\arcsin I,\frac{1}{2}-\frac{1}{2\pi}\arcsin I]$, then $Z(t)$ decreases in time approaching the stable fixed point. If the initial value $Z(0)$ falls into $[-\frac{1}{2}-\frac{1}{2\pi}\arcsin I,\frac{1}{2\pi}\arcsin I]$, then $Z(t)$ increases in time approaching the stable fixed point. It follows that there are upper and lower bounds on the change of $Z$.

$$\max\{Z(\infty)-Z(0)\}=\frac{1}{\pi}\arcsin I+\frac{1}{2},$$

$$\min\{Z(\infty)-Z(0)\}=\frac{1}{\pi}\arcsin I-\frac{1}{2}. \tag{5}$$

In order to solve nonlinear Eq. (3), one must consider different cases according to the values of $|Wr/FR+S_1|$ and $|Wr/FR+S_2|$.

For $|Wr/FR+S_1|<1$ and $|Wr/FR+S_2|<1$, $Z=\frac{1}{2\pi}\arcsin(Wr/FR+S_1)$ and $Z=\frac{1}{2\pi}\arcsin(Wr/FR+S_2)$ are stable fixed points for $0<\mathrm{mod}(T,T_1)<T_*$ and $T_*<\mathrm{mod}(T,T_1)<T_1$, respectively. The average velocity $\langle dZ/dT\rangle$ is zero. In other words

$$V_p=\left\langle\frac{dx}{dt}\right\rangle=0. \tag{6}$$

This case is not interesting from an experimental point of view, since the load $W$ has no net motion.

Now we consider the case where $|Wr/FR+S_1|>1$ and $|Wr/FR+S_2|<1$ [21]. We search for periodic solutions such that $Z(T_1)=Z(0)+n$, where $n$ is an integer. Then $\langle dZ/dT\rangle=n/T_1$ or

$$V_p=\left\langle\frac{dx}{dt}\right\rangle=-\frac{n}{T_1}\frac{\lambda}{\frac{\zeta\lambda}{FR^2}}. \tag{7}$$

The load $W$ has a net upward motion when $n<0$.

To find $n$, we use Eq. (4) to write $\tan(\omega_1T-\omega_1T_{01})=\frac{\pi}{\omega_1}[(\frac{Wr}{FR}+S_1)\tan(\pi Z)-1]$ for $0<\mathrm{mod}(T,T_1)<T_*$, where $T_{01}$ is an integration constant and $\omega_1=\pi\sqrt{(Wr/FR+S_1)^2-1}$. $T_{01}$ can be easily written in terms of $Z(0)$.

$$-\tan(\omega_1T_{01})=\frac{\pi}{\omega_1}\left[\left(\frac{Wr}{FR}+S_1\right)\tan(\pi Z(0))-1\right]. \tag{8}$$

We also get the following equation for $Z(T_*)$.

$$\tan(\omega_1T_*-\omega_1T_{01})=\frac{\pi}{\omega_1}\left\{\left(\frac{Wr}{FR}+S_1\right)\tan[\pi Z(T_*)]-1\right\}. \tag{9}$$

We find $\exp(2\omega_2T-2\omega_2T_{02})=\left|\frac{\tan\pi Z-\cot\pi Z_c}{\tan\pi Z-\tan\pi Z_c}\right|$ for $T_*<\mathrm{mod}(T,T_1)<T_1$. Here $2\pi Z_c=\arcsin(Wr/FR+S_2)$, $\omega_2=\pi\sqrt{1-(Wr/FR+S_2)^2}$, and integration constant $T_{02}$ can be written in terms of $Z(T_1)$. Now using the periodicity condition $Z(T_1)=Z(0)+n$, we find

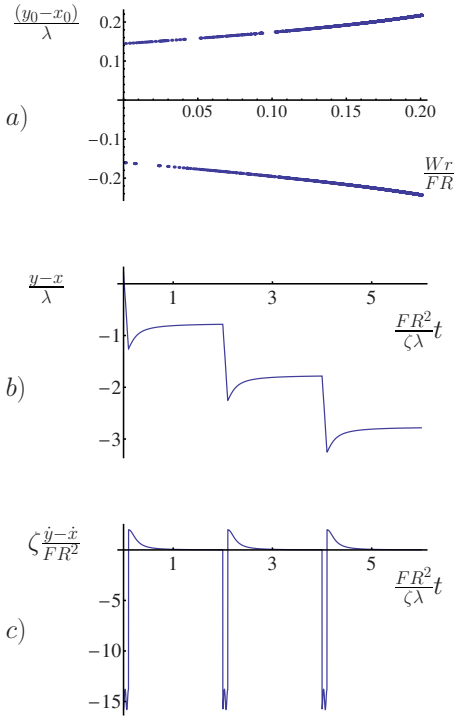


FIG. 2. (Color online) (a) Admissible values of $y_0-x_0$ in unit of $\lambda$ as a function of $Wr/(FR)$. Here $T_*=0.1$, $T_1=2$, and $S_1=-15$. It follows that $n=-1$ and $V_p=FR^2/(2\zeta)$. (b) $y-x$ in unit of $\lambda$ vs time in units of $\zeta\lambda/(FR^2)$, for $y_0-x_0=0.2169\lambda$ and $Wr=0.2FR$. (c) The velocity $dy/dt-dx/dt$ in units of $FR^2/\zeta$ as a function of time, for the same parameters.

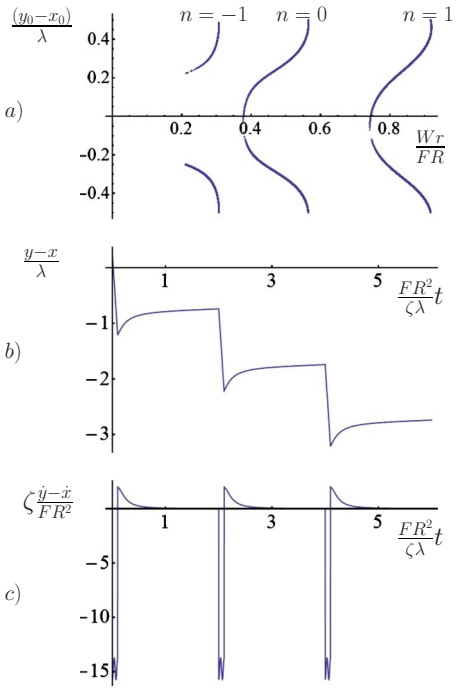


FIG. 3. (Color online) (a) Admissible values of $y_0-x_0$ in unit of λ as a function of $Wr/(FR)$. Here $T_*=0.1$, $T_1=2$, and $S_1=-15$. Three branches corresponding to $n=-1$, $n=0$, and $n=1$ are shown. In case of $n=-1$, the load $W$ acquires the upward velocity $V_p=FR^2/(2\zeta)$. (b) $y-x$ in unit of λ vs time in units of $\zeta\lambda/(FR^2)$, for $y_0-x_0=0.2603\lambda$ and $Wr=0.2537FR$. (c) The velocity $dy/dt-dx/dt$ in units of $FR^2/\zeta$ as a function of time, for the same parameters.

$$e^{2\omega_2(T_1-T_*)}=\frac{[\tan\pi Z(0)-\cot\pi Z_c][\tan\pi Z(T_*)-\tan\pi Z_c]}{[\tan\pi Z(0)-\tan\pi Z_c][\tan\pi Z(T_*)-\cot\pi Z_c]}. \tag{10}$$

For a given set of parameters $Wr/(FR)$, $T_*$, $T_1$, and $S_1$ we solve Eqs. (8)–(10) to find the admissible values of initial condition $Z(0)$. We obtain $n$ from the periodicity condition $Z(T_1)-Z(0)=n$. Note that for $0<T<T_*$, $\langle dZ/dT\rangle=\mathrm{sgn}(Wr/FR+S_1)\omega_1/\pi$, where $\mathrm{sgn}(x)=x/|x|$. Thus $Z(T_*)-Z(0)\simeq\mathrm{sgn}(Wr/FR+S_1)\omega_1T_*/\pi$. Equation (5) shows that $2Z_c-1/2<Z(T_1)-Z(T_*)<2Z_c+1/2$. The identity $Z(T_1)-Z(0)=[Z(T_*)-Z(0)]+[Z(T_1)-Z(T_*)]$ then allows us to find the integer $n$.

Following the procedure outlined above, we get the following set of equations when both $|Wr/FR+S_1|>1$ and $|Wr/FR+S_2|>1$:

$$-\tan(\omega_1T_{01})=\frac{\pi}{\omega_1}\left[\left(\frac{Wr}{FR}+S_1\right)\tan(\pi Z(0))-1\right],$$

$$\tan(\omega_1T_*-\omega_1T_{01})=\frac{\pi}{\omega_1}\left\{\left(\frac{Wr}{FR}+S_1\right)\tan[\pi Z(T_*)]-1\right\},$$

$$\tan(\omega_2'T_*-\omega_2'T_{02})=\frac{\pi}{\omega_2'}\left\{\left(\frac{Wr}{FR}+S_2\right)\tan[\pi Z(T_*)]-1\right\},$$

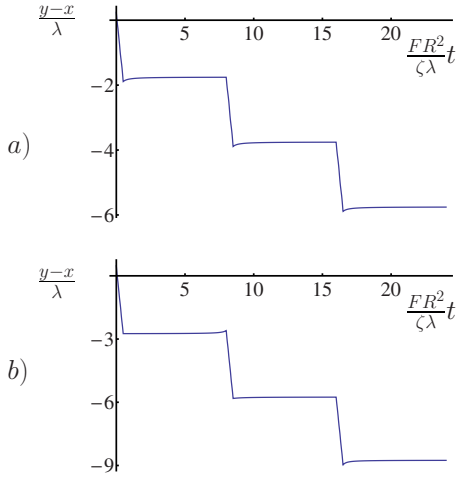


FIG. 4. (Color online) $y-x$ in unit of λ vs time in units of $\zeta\lambda/(FR^2)$. (a) For the parameters $T_*=0.5$, $T_1=8$, $S_1=-5$, $y_0-x_0=0.242\lambda$, and $Wr=0.666FR$, the signal shows that $n=-2$. (b) For the parameters $T_*=0.5$, $T_1=8$, $S_1=-7$, $y_0-x_0=0.475\lambda$, and $Wr=0.553FR$, the signal shows that $n=-3$.

$$\tan(\omega_2'T_1-\omega_2'T_{02})=\frac{\pi}{\omega_2'}\left\{\left(\frac{Wr}{FR}+S_2\right)\tan[\pi Z(0)]-1\right\}, \tag{11}$$

where $\omega_2'=\pi\sqrt{(Wr/FR+S_2)^2-1}$. For a given set of parameters, we solve the above set of equations to find the admissible values of $Z(0)$ and then obtain $n$ from the periodicity condition $Z(T_1)-Z(0)=n$.

## III. RESULTS

As an example, we consider the case of $T_*=0.1$, $T_1=2$, $S_1=-15$, and $S_2=15/19$. Figure 2(a) depicts the admissible values of $(y_0-x_0)/\lambda$ as a function of $Wr/(FR)$. Note that we have studied the region $Wr/(FR)<0.2$, thus $|Wr/FR+S_1|>1$ and $|Wr/FR+S_2|<1$. We find $n=-1$, in other words the load $W$ has a net *upward* velocity $V_p=FR^2/(2\zeta)$. For the parameters $y_0-x_0=0.2169\lambda$ and $Wr=0.2FR$, Figs. 2(b) and 2(c) show $y-x$ and $dy/dt-dx/dt$ as a function of time, respectively. This specific example shows clearly that $[y(T+T_1)-x(T+T_1)]/\lambda=[y(T)-x(T)]/\lambda-1$, hence $n=-1$.

Figure 3(a) depicts the admissible values of $(y_0-x_0)/\lambda$ as a function of $Wr/(FR)$ for $T_*=0.1$, $T_1=2$, $S_1=-15$, and $S_2=15/19$. Note that here we have studied the region $Wr/(FR)>0.2$, thus $|Wr/FR+S_1|>1$ and $|Wr/FR+S_2|>1$. Three branches corresponding to $n=-1$, $n=0$, and $n=1$ are shown. In case of $n=-1$, the load $W$ acquires the upward velocity $V_p=FR^2/(2\zeta)$. For the parameters $y_0-x_0=0.2603\lambda$ and $Wr=0.2537FR$, Figs. 3(b) and 3(c) show $y-x$ and $dy/dt-dx/dt$ as a function of time, respectively.

In our numerical investigations, we observed the solution $n=-1$ frequently. Quite remarkably, we observed $n=-2$ and $n=-3$ for specific values of parameters. We find $n=-2$ for $T_*=0.5$, $T_1=8$, $S_1=-5$, $y_0-x_0=0.242\lambda$, and $Wr=0.666FR$. We also find $n=-3$ for $T_*=0.5$, $T_1=8$, $S_1=-7$, $y_0-x_0=0.475\lambda$ and $Wr=0.553FR$, see Fig. 4.

## IV. DISCUSSION

The pinion is mounted on an axle. We assume that the friction in the system comes from the lubrication at the axle. For an axle lubricated with a fluid layer of thickness $h$ and viscosity $\eta$, we find $\zeta \simeq 2\pi\eta L r^3/h$, where $L$ is the height of the pinion and $r$ is the radius of the axle [10]. Using $\eta = 10^{-3}$ Pa s for a lubricant as thick as water, $L = 10$ $\mu$m, $r = 500$ nm, and $h = 100$ nm, we find $\zeta = 7.85 \times 10^{-20}$ kg m$^2$/s.

For typical and experimentally realizable values of $a_r = a_p = 50$ nm, $R = 1$ $\mu$m, and $\lambda = 500$ nm, we find $F = 0.3$ pN for $H = 200$ nm [8]. The pinion rotates with an angular velocity $\Omega = V_P/R = -nFR/(T_1\zeta)$. For the first example presented before, $n = -1$, $T_1 = 2$ and hence $\Omega = 1.91$ Hz. However, reducing the gap size by only a factor of two to $H = 100$ nm yields $F = 12$ pN and consequently $\Omega = 76.43$ Hz.

Inspired by the recent measurements of the lateral Casimir force [6], we believe that the rack and pinion device is realizable with the currently available technologies. Using the typical values of geometric parameters, and assuming that the rack position versus time is a periodic triangular signal, we find that the pinion rotates with an average angular velocity $\Omega = 1 \sim 100$ Hz. Experimental observation of the pinion rotation will show that the quantum vacuum can intermesh the noncontact parts of nanomachines.

Our work can be extended in many directions. Here we have assumed that the temperature of the system is zero and the external noises are absent. One can use the Langevin equation to describe the pinion motion under the influence of thermal noises [7]. The impact of external mechanical noises and random vibrations on the system deserves a detailed study. A question of interest is whether the device can rectify random motions of the rack.


[1] H. B. G. Casimir, Proc. K. Ned. Akad. Wet. **51**, 793 (1948).

[2] M. Bordag, G. L. Klimchitskaya, U. Mohideen, and V. M. Mostepanenko, *Advances in the Casimir Effect* (Oxford University Press, Oxford, 2009).

[3] H. B. Chan, V. A. Aksyuk, R. N. Kleiman, D. J. Bishop, and F. Capasso, Science **291**, 1941 (2001); Phys. Rev. Lett. **87**, 211801 (2001).

[4] R. Golestanian and M. Kardar, Phys. Rev. Lett. **78**, 3421 (1997).

[5] T. Emig, A. Hanke, R. Golestanian, and M. Kardar, Phys. Rev. A **67**, 022114 (2003).

[6] F. Chen, U. Mohideen, G. L. Klimchitskaya, and V. M. Mostepanenko, Phys. Rev. Lett. **88**, 101801 (2002); Phys. Rev. A **66**, 032113 (2002).

[7] T. Emig, Phys. Rev. Lett. **98**, 160801 (2007).

[8] A. Ashourvan, M. F. Miri, and R. Golestanian, Phys. Rev. Lett. **98**, 140801 (2007).

[9] A. Ashourvan, M. F. Miri, and R. Golestanian, Phys. Rev. E **75**, 040103(R) (2007).

[10] M. F. Miri and R. Golestanian, Appl. Phys. Lett. **92**, 113103 (2008).

[11] M. F. Miri, V. Nekouie, and R. Golestanian, Phys. Rev. E **81**, 016104 (2010).

[12] E. Buks and M. L. Roukes, Phys. Rev. B **63**, 033402 (2001); M. P. de Boer and T. M. Mayer, MRS Bull. **26**, 302 (2001); A. Socoliuc, E. Gnecco, S. Maier, O. Pfeiffer, A. Baratoff, R. Bennewitz, and E. Meyer, Science **313**, 207 (2006); J. Y. Park, D. F. Ogletree, P. A. Thiel, and M. Salmeron, *ibid.* **313**, 186 (2006); R. W. Carpick, *ibid.* **313**, 184 (2006); J. A. Williams and H. R. Le, J. Phys. D **39**, R201 (2006).

[13] A. Azari, H. S. Samanta, and R. Golestanian, New J. Phys. **11**, 093023 (2009).

[14] A. Lambrecht and V. N. Marachevsky, Phys. Rev. Lett. **101**, 160403 (2008).

[15] I. Cavero-Peláez, K. A. Milton, P. Parashar, and K. V. Shajesh, Phys. Rev. D **78**, 065018 (2008); **78**, 065019 (2008).

[16] F. C. Lombardo, F. D. Mazzitelli, and P. I. Villar, J. Phys. A **41**, 164009 (2008).

[17] S. Y. Buhmann, S. Scheel, and J. Babington, Phys. Rev. Lett. **104**, 070404 (2010).

[18] H. C. Chiu, G. L. Klimchitskaya, V. N. Marachevsky, V. M. Mostepanenko, and U. Mohideen, Phys. Rev. B **81**, 115417 (2010).

[19] Here int$(T/T_1)$ denotes conversion of real number $T/T_1$ to integer by truncation. mod$(T,T_1) = T/T_1 - \text{int}(T/T_1)$.

[20] J. Kim, A. Sosso, and A. F. Clark, J. Appl. Phys. **83**, 3225 (1998).

[21] By a suitable choice of origin for time, one obtains similar results in case of $|Wr/FR + S_1| < 1$ and $|Wr/FR + S_2| > 1$.